An Improved Computational Method for Noise Parameter Measurement

MASATAKA MITAMA, MEMBER, IEEE, AND HIDEHIKO KATOH

***Abstract*—Conventional methods for noise parameter measurement for linear noisy two-ports have been improved by introducing a computational method for evaluating measured admittance errors. Derivation and comparison with a conventional method are given. Noise parameters of a packaged 0.5-μm gate-length GaAs MESFET (NE38806) were successfully measured using the proposed technique.**

I. Introduction

As IS WELL KNOWN, the noise behavior of a linear noisy two-port network can be characterized by the four noise parameters, F_0, G_0, B_0, and R_n, as

$$F=F_0+\frac{R_n}{G_s}\left\{(G_s-G_0)^2+(B_s-B_0)^2\right\} \tag{1}$$

where

- F noise figure,
- Y_s $G_s+jB_s=$source admittance,
- F_0 minimum noise figure,
- Y_0 $G_0+jB_0=$optimum source admittance that gives minimum noise figure,
- R_n equivalent noise resistance.

The usual method [1] of obtaining noise parameters requires a special source admittance setting procedure, which is tedious.

An alternate method [2] consists of performing noise figure measurements for more than four arbitrary source admittances with a least squares method used for data processing. In this method, an estimated error (residue) ϵ_i' is defined for the ith measured data set (G_{si},B_{si},F_i) $(i=1,2,\cdots,N)$ as

$$\epsilon_i'=\left|F_0+\frac{R_n}{G_{si}}\left\{(G_{si}-G_0)^2+(B_{si}-B_0)^2\right\}-F_i\right| \tag{2}$$

which is shown by the dotted line ϵ_i' in Fig. 1. The weighted square sum of the estimated error is minimized. However, of the three measurement values G_{si}, B_{si}, and F_i, (2) considers the measured error in F only. That is, no consideration is made for measured G_s and B_s errors. Thus measured F errors at Y_s values away from Y_0 tend to be overvaluated, resulting in unsatisfactory computed noise parameter values, especially at higher microwave frequencies. In particular, according to Lane [2], computed results are highly sensitive to measurement errors in case of a large R_n.

Manuscript received September 7, 1978; revised January 2, 1979.

The authors are with the Central Research Laboratories, Nippon Electric Company, Ltd., 4-Miyazaki, Takatsu-ku, Kawasaki 213, Japan.

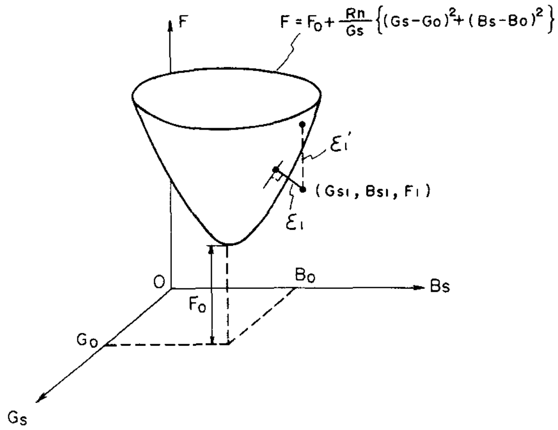

Fig. 1. Estimated error ϵ_i for the present least squares method. The dashed line designated by ϵ_i' represents the corresponding error used in the conventional method [2].

Assigning weighting values according to each measurement accuracy has been suggested [3], but is deemed impractical.

In the present paper, a computational method is introduced for evaluating measured source admittance errors, as well as the measured F error.

Another reason for unsatisfactory results with the conventional methods is the random differences between measured Y_s values and actual Y_s values imposed onto the two-port network. In the present method, a low-loss microstrip tuner is used, which helps to decrease the errors introduced by these differences.

II. Least Squares Method Considering Y_s Errors

Let $G_s=x$, $B_s=y$, $F=z$, $F_0=a_1$, $R_n=a_2$, $G_0=a_3$, and $B_0=a_4$ for simplicity of notation. Let the estimated values for the measured set (X_i,Y_i,Z_i) $(i=1,2,\cdots,N)$ in the x, y, and z coordinates be $(\hat{x}_i,\hat{y}_i,\hat{z}_i)$ and the estimated values for parameters a_1, a_2, a_3, and a_4 be $\hat{a}_1$, $\hat{a}_2$, $\hat{a}_3$, and $\hat{a}_4$. Furthermore, define the estimated errors (residues) as

$$V_{xi}=\hat{x}_i-X_i \quad V_{yi}=\hat{y}_i-Y_i \quad V_{zi}=\hat{z}_i-Z_i \tag{3}$$

$$V_{a1}=\hat{a}_1-a_1^0 \quad V_{a2}=\hat{a}_2-a_2^0 \quad V_{a3}=\hat{a}_3-a_3^0 \quad V_{a4}=\hat{a}_4-a_4^0 \tag{4}$$

where a_1^0, a_2^0, a_3^0, and a_4^0 are zeroth-order approximation values. These estimated values must satisfy the functional relation of

$$G(\hat{x}_i,\hat{y}_i,\hat{z}_i;\hat{a}_1,\hat{a}_2,\hat{a}_3,\hat{a}_4)=0, \qquad i=1,2,\cdots,N \tag{5}$$

0018-9480/79/0600-0611$00.75 ©1979 IEEE

where

$$G(x,y,z;a_1,a_2,a_3,a_4) = -z + a_1 + \frac{a_2}{x}\left\{(x-a_3)^2+(y-a_4)^2\right\}. \quad (6)$$

Equation (6) is derived by transposing the left-hand side value of (1) to the right-hand side values.

The term "estimated values" is defined such that $x_i, \cdots, a_4$ minimize

$$S = \sum_i \left(w_{xi}V_{xi}^2 + w_{yi}V_{yi}^2 + w_{zi}V_{zi}^2\right)_{\min} \quad (7)$$

where w_{xi}, w_{yi}, and w_{zi} are weights to be determined according to measurement accuracies, and the subscript min denotes the minimum value within the parentheses.

When $w_{xi} = w_{yi} = w_{zi} = 1$, the quantity

$$\epsilon_i = \left\{\left(w_{xi}V_{xi}^2 + w_{yi}V_{yi}^2 + w_{zi}V_{zi}^2\right)_{\min}\right\}^{1/2} \quad (8)$$

represents the length of a segment of a line normal to the quasi-elliptic paraboloid represented by (5) projected from the measured point (X_i, Y_i, Z_i), as shown by the solid line ϵ_i in Fig. 1.

Note that the minimum value within the parentheses in (7) occurs when the line drawn from the measured point is perpendicular to the quasi-elliptic paraboloid. With (8), the evaluation of the measured Y_s error as well as that of the measured F error becomes possible, as contrasted to the conventional method [2].

Assuming that estimated errors are small, (5) can be expanded in a Taylor series to a first-order approximation as

$$G_0^i + G_x^i V_{xi} + G_y^i V_{yi} + G_z^i V_{zi} + G_{a1}^i V_{a1} + G_{a2}^i V_{a2} + G_{a3}^i V_{a3} + G_{a4}^i V_{a4} = 0 \quad (9)$$

where

$$G_0^i = G\left(X_i, Y_i, Z_i; a_1^0, a_2^0, a_3^0, a_4^0\right) \quad (10)$$

$$G_x^i = \left.\frac{\partial G}{\partial x}\right|_{x=X_i, y=Y_i, z=Z_i; a_1=a_1^0, a_2=a_2^0, a_3=a_3^0, a_4=a_4^0} \quad (11)$$

and $G_y^i, \cdots, G_{a4}^i$ are similar to the above. Using (9), (8) can be rewritten as

$$\epsilon_i = \sqrt{w_i}\,|d_i| \quad (12)$$

where

$$d_i = -\left(G_{a1}^i V_{a1} + G_{a2}^i V_{a2} + G_{a3}^i V_{a3} + G_{a4}^i V_{a4} + G_0^i\right) \quad (13)$$

$$1/w_i = \left(G_x^i\right)^2/w_x + \left(G_y^i\right)^2/w_y + \left(G_z^i\right)^2/w_z. \quad (14)$$

The derivation of (12) is shown in the Appendix.

Then, by the least squares method, a set of linear equations is obtained as

$$\frac{\partial S}{\partial V_{a1}} = 2\sum_i \left[w_i d_i G_{a1}^i\right] = 0$$

$$\vdots$$

$$\frac{\partial S}{\partial V_{a4}} = 2\sum_i \left[w_i d_i G_{a4}^i\right] = 0. \quad (15)$$

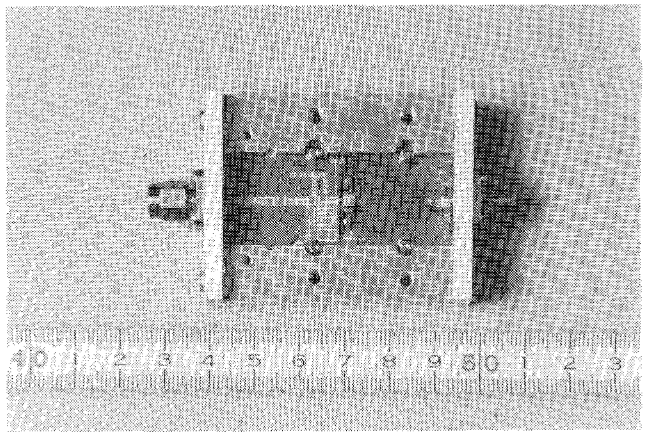

Fig. 2. Microstrip tuner.

In order to solve (15), the initial values a_1^0, a_2^0, a_3^0, and a_4^0 were obtained by using the conventional method described in [2]. Then (15) was solved by an iteration method using (3) and (4) to obtain the V_{a1}, V_{a2}, V_{a3}, and V_{a4} that make S minimum. In the present calculation, w_{xi}, w_{yi}, and w_{zi} were set to unity.

III. Measurement

A. Microstrip Tuner

Usually, commercial stub tuners are widely used to provide Y_s values necessary for noise parameter measurements. However, good reproducibility is difficult to obtain with these stub tuners. In addition, dissipation loss must be calibrated for each Y_s value, which is tedious. To avoid these requirements, an integrated microstrip tuner, shown in Fig. 2, has been used. To a 50-Ω main line, eight open shunt stubs (lands) were constructed on a 0.8-mm-thick teflon-glass fabric board (Di Clad 522). Each stub consisted of ten 0.8-mm × 1-mm lands with 0.2-mm separation. By connecting appropriate lands with an adhesive conductive sheet, necessary Y_s values can be obtained on an arbitrary basis. Y_s values were recorded with an $X-Y$ recorder prior to the noise figure measurement. Fig. 3 shows an example. Circles in the figure indicate the source admittance points realized. Each solid line shows the locus of discrete change of the source admittance when one particular stub length is adjusted by connecting the lands one by one with an adhesive conductive sheet. The reproducibility using this arrangement was superior to that using a stub tuner. The dissipation loss, calculated by using generalized scattering matrices [4], was 0.02 dB for the particular Y_0 circuit configuration; hence the circuit loss was neglected throughout.

B. Available Gain

In order to minimize the Y_s value inaccuracy caused by connector disconnection, a two-port network available gain was calculated using both the premeasured Y_s value and the two-port network S parameters. Since circuit losses will result in an actual available gain smaller than that computed, receiving system noise contribution will not be overevaluated. The output matching circuit con-

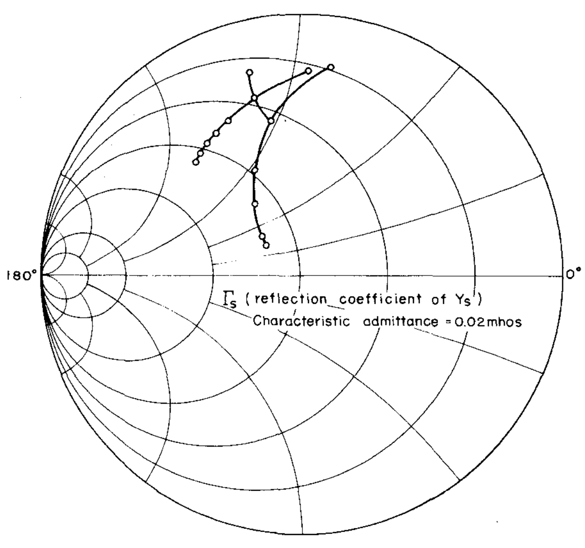

Fig. 3. An example of source admittance ($f=6$ GHz).

sisted of two quarter-wave transformer sections, common throughout the measurement, with less than 2.5 output VSWR. In a unilateral two-port network case, as is the case of an FET, the input impedance of the two-port network can be considered as being independent of the load impedance. Output circuit loss was neglected throughout.

C. NF Measurement

Noise figure (NF) measurements were made at 6, 7, and 8 GHz with an HP 342A automatic NF meter for a packaged 0.5-μm gate-length GaAs MESFET (NE 38806). To reduce the receiving system noise contribution, a low-noise preamplifier (NF < 3 dB, Gain > 17 dB) was placed directly after the FET output matching circuit. Although the measured NF was the double-sideband (signal and image) value, it can be considered as a single-sideband value, since signal and image separation is only 60 MHz.

IV. Calculation Results

A. Comparison with Conventional Method

In Fig. 4, the computed noise parameter standard deviation as a function of the number of measurement points N is shown both for the present and for the conventional method [2]. For each N, ten different trains of data sets were randomly selected from a total of fourteen measured points. Then, noise parameters and standard deviations were calculated for each N case. The figure shows that a smaller noise parameter deviation is obtainable with the present method for any given number of measurement points. Fig. 5 shows computed noise parameter sensitivities to an individual data set (G_{si}, B_{si}, F_i) accuracy. Noise parameters are calculated by extracting each data set one by one sequentially from fourteen data sets. It is clear that the individually measured data is less sensitive to the computed parameters with the present method. The small deviation in computed noise parameters and the insensitivity to individual data with the present method should be attributable to the new estimated error evaluation method described in Section II.

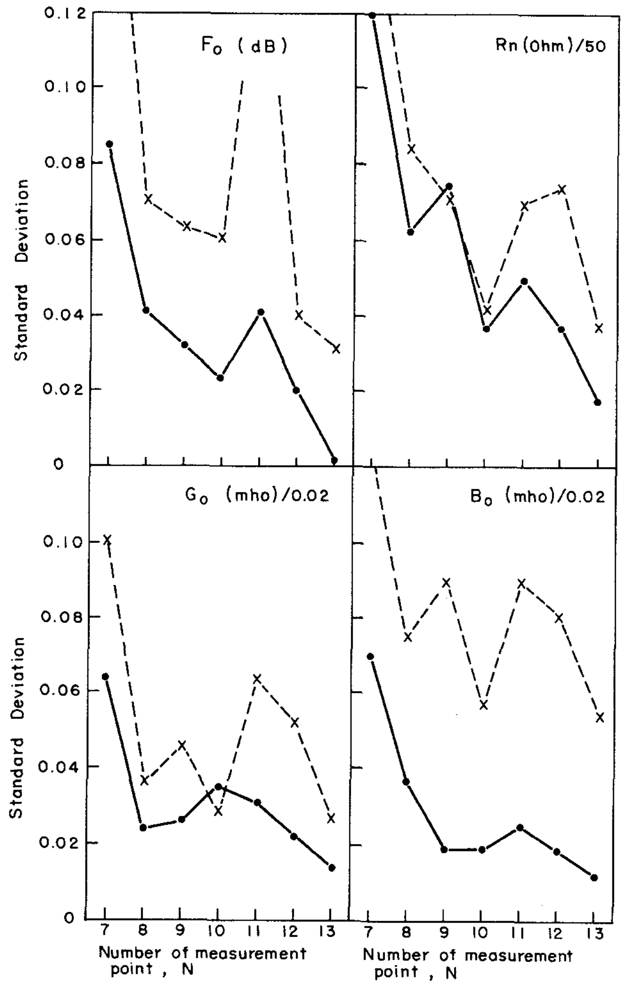

Fig. 4. Computed noise parameter standard deviation comparison with conventional method ($f=6$ GHz) [2]. The solid line curve corresponds to the present method, while the dashed line curve corresponds to the conventional method.

TABLE I
NOISE PARAMETERS OF A 0.5-μm GATE-LENGTH GAAS MESFET (NE 38806 OR 2SK124). $V_p=-2.21$ V, $I_{DSS}=51$ mA

FET	I_{DS} (mA)	V_{DS} (V)	f (GHz)	F_o (dB)	$\lvert\Gamma_o\rvert$	ϕ_o (deg.)	Rn/50 (ohm)
NE 38806	10	3	6	1.88	0.660	114.3	0.53
"	"	"	7	1.93	0.642	140.2	0.30
"	"	"	8	2.10	0.592	164.0	0.12

B. Measured Noise Parameters for NE 38806

Noise parameters for a packaged 0.5-μm gate-length GaAs MESFET (NE 38806) were measured with the present method. Results are listed in Table I. Measurement points for 6, 7, and 8 GHz were 14, 13, and 15, respectively. Because of rather small R_n values, 26.5–6 Ω, constant noise figure circles [5] indicated a mild dependence on Γ_s (reflection coefficient of Y_s) planes.

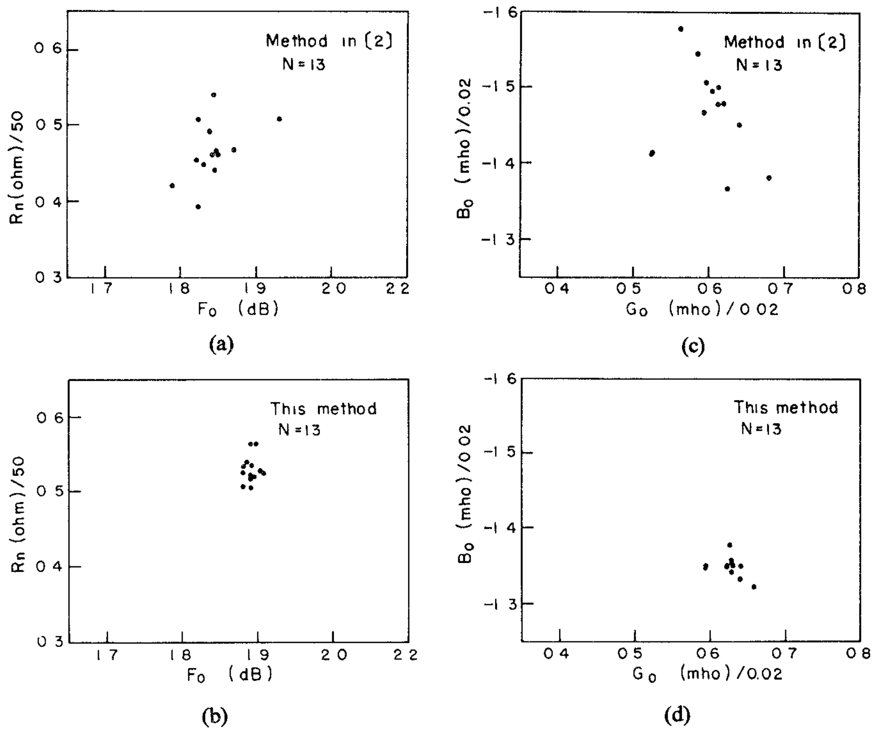

Fig. 5. Comparison of the sensitivity in computed noise parameters to individual data ($f=6$ GHz). (a) and (c) are the conventional method [2]; (b) and (d) are the present method.

V. Conclusion

Conventional methods [1], [2] for noise parameter measurement have been improved by introducing a new computational method for evaluating measured source admittance errors as well as the measured noise figure error and by utilizing an integrated microstrip tuner. It was demonstrated that a smaller deviation in the computed noise parameters and insensitivity to individual data were achieved with the present method when compared with the conventional method [2]. Noise parameters of a packaged 0.5-μm gate-length GaAs MESFET (NE 38806) have been successfully measured with the new method.

Appendix
Derivation of (12)

Consider the terms within the parentheses of (8),

$$s_{hi}=w_{xi}V_{xi}^2+w_{yi}V_{yi}^2+w_{zi}V_{zi}^2. \tag{A.1}$$

In the following, the superscripts and subscripts i's are dropped throughout for simplicity. Using (9) and (13), (A.1) can be rewritten as

$$s_h=w_xV_x^2+w_yV_y^2+\frac{w_z}{G_z^2}(d-G_xV_x-G_yV_y)^2. \tag{A.2}$$

The minimum of s_h occurs when $\partial s_h/\partial V_x=0$ and $\partial s_h/\partial V_y=0$, simultaneously. Thus we obtain a set of linear equations as

$$\left(w_x+w_z\frac{G_x^2}{G_z^2}\right)V_x+\left(w_z\frac{G_xG_y}{G_z^2}\right)V_y=\left(w_z\frac{G_x}{G_z^2}\right)d \tag{A.3}$$

$$\left(w_z\frac{G_xG_y}{G_z^2}\right)V_x+\left(w_y+w_z\frac{G_y^2}{G_z^2}\right)V_y=\left(w_z\frac{G_y}{G_z^2}\right)d. \tag{A.4}$$

Solving (A.3) and (A.4), we obtain

$$V_x=w\left(\frac{G_x}{w_x}\right)d \quad V_y=w\left(\frac{G_y}{w_y}\right)d \quad \text{and } V_z=w\left(\frac{G_z}{w_z}\right)d. \tag{A.5}$$

Then, from (A.1) and (A.5), we have

$$\epsilon=\sqrt{(s_h)_{\min}}=\sqrt{w}\,|d|.$$

Acknowledgment

The authors would like to thank Dr. K. Ayaki and the members of the Microwave Circuit Group, Central Research Laboratories, Nippon Electric Company, Ltd., for their encouragement and guidance.

References

[1] IRE Subcommittee on Noise, "IRE standards on methods of measuring noise in linear twoports, 1959," *Proc. IRE*, vol. 48, pp. 60–68, Jan. 1960.
[2] R. Q. Lane, "The determination of device noise parameters," *Proc. IEEE*, vol. 57, pp. 1461–1462, Aug. 1969.
[3] M. S. Gupta, "Determination of the noise parameters of a linear 2-port," *Electron. Lett.*, vol. 6, pp. 543–544, Aug. 20, 1970.
[4] G. E. Bodway, "Two port power flow analysis using generalized scattering parameters," *Microwave J.*, vol. 10, pp. 61–69, May 1967.
[5] H. Fukui, "Available power gain, noise figure, and noise measure of two-ports and their graphical representations," *IEEE Trans. Circuit Theory*, vol. CT-13, pp. 137–142, June 1966.